Available online at www.sciencedirect.com
SCIENCE DIRECT®
Thermochimica Acta 423 (2004) 127–135
thermochimica acta
www.elsevier.com/locate/tca

Thermal history effects on crystallisation and melting of poly(3-hydroxybutyrate)

L.M.W.K. Gunaratne, R.A. Shanks*, G. Amarasinghe

School of Applied Science, RMIT University, GPO Box 2476V, Melbourne, Vic. 3001, Australia

Received 17 March 2004; received in revised form 29 April 2004; accepted 5 May 2004
Available online 24 June 2004

Abstract

The effect of thermal history on morphology, melting and crystallisation behaviour of bacterial poly(3-hydoxybutyrate) (PHB) have been investigated by using differential scanning calorimetry (DSC), temperature modulated DSC (TMDSC) and hot stage optical microscopy (HSOM). Various thermal histories were imparted by crystallisation with different continuous and modulated cooling techniques that involve cool–heat and cool–isothermal segments. The subsequent melting behaviour revealed that all samples experienced secondary crystallisation during heating and the extent of secondary crystallisation was varied depending on the treatment. PHB samples crystallised under slow to moderate continuous cooling rates were found to exhibit double melting behaviour due to melting of DSC scan-induced secondary crystals, but to a lesser extent. Samples subjected to a fast cooling rate gave amorphous PHB, while considerable secondary crystallisation/annealing took place under modulated cooling conditions. Additionally, the effect of melting conditions was also investigated by applying various continuous and modulated programs. The overall melting behaviour was rationalised in terms of recrystallisation and/or annealing of crystals. Interestingly, the samples analysed by temperature modulation programs showed a broad exotherm before the melting peak in the non-reversing curve and a multiple melting reversing curve, verifying that the melting–recrystallisation and remelting process is also operative. HSOM studies supported that the radial growth rate of the PHB spherulites was significantly varied upon the crystallisation conditions.

Keywords: Poly(3-hydroxybutyrate); Step-scan DSC; TMDSC; Melting; Crystallisation

1. Introduction

Poly(3-hydroxybutyrate) (PHB) is a biopolyester having a chemical structure of $[–O–CH–(CH_3)–CH_2–(C=O)–]_n$. PHB was first discovered in 1925 by Lemoigne [1]. PHB is usually produced by bacterial fermentation, and it has attracted enormous attention in agricultural, pharmaceutical and medical industry due to its biocompatibility and biodegradability. Since PHB degrades in all environments, it has been widely used in the packaging industry as a biodegradable polymer to minimise environmental pollution. PHB is a controversial polymer with many interesting characteristics. It's continuing interest as a commercial biopolymer and its various thermal and mechanical properties have made the subject of many studies [1–5]. PHB is a highly crystalline thermoplastic polymer with a relatively high melting temperature (in the range of 170–180 °C) and a glass transition temperature in the range of 0–5 °C. It undergoes thermal degradation at temperatures around the melting temperature [2,6]. PHB of natural origin has perfect stereoregularity, high purity and high degree of crystallinity so that it has been considered as a model polymer to study crystallisation and morphology [7]. PHB has low nucleation density and crystallises slowly to form large spherulites [8].

Differential scanning calorimetry (DSC) has been a vital technique to study melting and crystallisation behaviour and the morphology of polymers. However, the interpretation of a DSC scan is often dubious due to various underlying transformations (recrystallisation, reorganisation and annealing) simultaneously occurring during heating. Temperature modulated differential scanning calorimetry (TMDSC) techniques, such as modulated differential scanning calorimetry (MDSC) and step-scan differential

* Corresponding author. Tel.: +61-3-9925-2122; fax: +61-3-9925-2122/+61-3-9639-1321.
E-mail address: robert.shanks@rmit.edu.au (R.A. Shanks).

0040-6031/$ – see front matter © 2004 Elsevier B.V. All rights reserved.
doi:10.1016/j.tca.2004.05.003

scanning calorimetry (SSDSC) have been established over the past few years as an alternative technique to produce new and different information on thermal transition of polymers relative to conventional DSC [9–11]. Its theory and operating principles are extensively described elsewhere [9–14]. TMDSC uses a periodical temperature modulation (sinusoidal, iso-scan and heat–cool) over a traditional linear heating or cooling ramp and is capable of giving accurate heat capacity measurements and separating underlying kinetic and thermodynamic phenomena with better resolution and sensitivity. For all modulations, the time temperature (t–T) program can be written as a sum of linear and periodic parts (T_p):

$$T(t) = T_0 + \beta_0 t + T_p(t)$$

where T_o is the initial temperature and β_0 the average heating rate.

In these experiments, there are two main methods to analyse the resulting modulated heat flow: reversing/non-reversing (NR) total heat flow or heat capacity approach as described by Reading and coworkers [9] and complex heat capacity approach by Schawe [10]. Despite the method used, three types of curves can normally be derived from the modulated DSC experiments: total heat flow or heat capacity curve (total C_p, same as conventional DSC curve), *in-phase* curve (reversing or storage) and *out-of-phase* curve (kinetic or loss) [15,16]. In addition, the non-reversing heat capacity curve (NRC_p) can be obtained by the difference between the total C_p and reversing heat capacity (C'_p). This curve is particularly useful for determining irreversible processes such as enthalpy relaxation, evaporation, cold crystallisation, chemical reactions, curing, decomposition and recrystallisation. The reversing curve represents the effects that are thermodynamically reversible at the time and temperature at which they are detected, whereas the *out-of-phase* curve is expected to show irreversible phenomena within the modulation conditions.

SSDSC technique has recently become available and developed as a simplified version to MDSC [17]. It utilises a heat–isothermal (or cooling–isothermal) program, where the isothermal segment continues until the heat flow is decreased to within a predetermined set-value (criteria). The thermodynamic response only occurs during the heating (or cooling) segment and reflects the reversible changes of the sample. The kinetic response yields the kinetic processes and extracts from the isothermal segment. The equation that describes the heat flow response is given by $dQ/dt = C_p(dT/dt) + f(t, T)$, where dQ/dt is the heat flow, C_p the heat capacity, dT/dt the heating rate and $f(t, T)$ the kinetic response. The interpretation of results is similar to the MDSC, and the reversing (thermodynamic C_p signal, reversible under the experimental conditions) and non-reversing (Isok baseline, kinetic) contributions can be directly extracted from data.

Since PHB is slow to reach crystallisation equilibrium, its thermal history can be readily controlled by its crystallisation conditions. PHB is brittle in nature. de Koning et al. have shown that it can also undergo physical ageing during the storage at room temperature increasing the brittleness [18]. The phenomenon of secondary crystallisation of initially formed crystals has been suggested, and researchers have also shown that PHB can be toughened by annealing [18,19] and crack-free spherulites can be grown from the melt by controlling the crystallisation conditions [20]. Investigation of non-isothermal crystallisation behaviour is important during the industrial processes, such as extrusion and moulding. In this paper, the influence of thermal history is explored using a range of non-isothermal crystallisation conditions, including modulated cooling programs. The melting of PHB is studied using continuous fast and slow heating, as well as TMDSC and step-scan conditions. A morphological study of PHB is carried out using HSOM with different crystallisation conditions related to the DSC cooling treatments.

2. Experimental

2.1. Sample preparation

Bacterial PHB was obtained from Sigma Aldrich Chemicals, Australia, as a white powder ($M_w = 2.3 \times 10^5$ g mol^{-1} and $M_n = 8.7 \times 10^4$ g mol^{-1} [21]). PHB (1 g) was dissolved in 100 mL of chloroform and filtered by vacuum filtration to remove the insoluble fraction or impurities. Semi-crystalline films were obtained by solvent casting at room temperature. The resulting films (~60 μm thick) were further dried in vacuum at 50 °C for 3 h to remove residual solvent and moisture. Films were stored in a desiccator under nitrogen atmosphere prior to use.

2.2. Differential scanning calorimetry

All thermal treatments and measurements were performed in a Perkin-Elmer Pyris 1 DSC (Pyris software 3.81) operated at subambient temperature mode with an Intracooler. In the Perkin-Elmer DDSC, iso-scan, heat–cool and step-scan modes are available. About 2–3 mg of sample was sealed in a 10 μL aluminium pan, and all scans were carried out under inert nitrogen (20 mL min^{-1}). High purity indium and octadecane were used for temperature calibration and indium standard was used for calibration of heat flow. Furnace calibration was performed according to the manufacturer instructions.

Samples were treated at different crystallisation conditions: continuous cooling at rates of 2, 10 and 200 °C min^{-1} from 190 to −20 °C and modulated cooling using both cool–heat, iso-scan modes at an average rate of 2 °C min^{-1}. Before the treatment, all samples were melted at 190 °C for 5 min to destroy any previous thermal history. In order to avoid thermal decomposition during temperature modulation at higher temperatures, the samples were rapidly cooled

to 140 °C from 190 °C at a nominal rate of 100 °C min^{-1} and held for 2 min. The modulated cooling program was then immediately followed from 140 to −20 °C. The cool–heat program used linear segments of cooling and heating with cooling rate of 6 °C min^{-1} for 30 s followed by heating at 2 °C min^{-1} for 30 s, respectively. The iso-scan program was of linear segments of cooling and isothermal with a cooling rate of 4 °C min^{-1} for 30 s followed by isothermal for 30 s. Both of these programs provided a frequency of 16.7 mHz (period = 60 s), an average cooling rate of 2 °C min^{-1} and a temperature amplitude of 1 °C for cool–heat and 0.5 °C for iso-scan. Standard DSC melting scans of the treated samples were then obtained from −20 to 190 °C at a rate of 10 °C min^{-1}. From the DSC melting scans, glass transition temperature (T_g), cold crystallisation temperature (T_{cc}), melting temperature (T_m) and enthalpy of fusion (ΔH_m) were determined. Crystallisation temperature (98.2 °C) and onset of crystallisation temperature (109.4 °C) were determined from DSC cooling scan obtained at 10 °C min^{-1} rate.

TMDSC melting scans were obtained by using a heat–cool and iso-scan modulation from −20 to 190 °C. As explained above, heat–cool and iso-scan melting scans were performed at an average rate of 2 °C min^{-1} heating rate with a period of 60 s and modulation amplitudes of 1 and 0.5 °C, respectively. The heat flow data from the TMDSC scans were then used to calculate the total heat capacity (total C_p), storage heat capacity (C'_p) and loss heat capacity (C''_p). The non-reversing heat capacity (NRC$_p$) curve was obtained by subtracting the C'_p curve from total C_p curve. The step-scan DSC melting scans of treated samples were obtained with the same average heating rate of 2 °C min^{-1} with a period of 60 s (temperature increment of 2 °C with each 30 s isothermal and scanning segments) from −20 to 190 °C. Specific heat calculation for heat flow response was carried out considering the area. The data points for isothermal segment were collected within the 0.05 mW s^{-1} criteria value. For each type of scan, a baseline was recorded with matched empty aluminium pans using the same methods. All standard DSC and TMDSC and SSDSC curves were corrected using the appropriate baselines recorded under identical conditions and converted to specific heat capacity curves. The crystallinity was calculated using the equation:

$$X_{\mathrm{cPHB}} = \frac{\Delta H_{\mathrm{PHB}}}{\Delta H^0_{\mathrm{PHB}}}$$

where $\Delta H^0_{\mathrm{PHB}}$ is the enthalpy of melting of pure crystals 146 J g^{-1} [22] and ΔH_{PHB} the measured enthalpy of melting for PHB.

2.3. Optical microscopy

The morphologies of PHB films were observed using a Nikon Labophot 2 polarised optical microscope with a Mettler FP90 hot stage and images were captured using Nikon digital camera. The solvent cast PHB films were mounted on glass slides and covered by cover slips. The specimens were first heated on a hot stage from room temperature to 190 °C at a rate of 5 °C min^{-1} and maintained at this temperature for 3 min before cooling. The morphological study of PHB was carried out using four different crystallisation conditions: isothermal crystallisation, continuous slow and fast cooling rates from 140 °C to room temperature and three-step crystallisation under a nitrogen atmosphere. Isothermal crystallisation behaviour was observed by maintaining the sample for 1 h at 80 °C after cooling at a rate of 5 °C min^{-1} from 190 °C. The cooling rates of 10 and 2 °C min^{-1} were used to provide analogues behaviour to the DSC treatment of polymers. The three-step crystallisation was performed by keeping samples for 5 min at 140, 120 and 90 °C after cooling to 140 °C at 5 °C min^{-1} rate and followed by 20 °C min^{-1} from 140 to 120 and 120–90 °C. This crystallisation method was used to provide a step-wise isothermal program analogous to the iso-scan cooling program in the TMDSC but with larger steps.

3. Results and discussion

3.1. Effect of crystallisation conditions

Fig. 1 shows the standard DSC melting scans of PHB obtained at a rate of 10 °C min^{-1} after various crystallisation treatments. These samples were crystallised by continuous cooling rates at 200, 10 and 2 °C min^{-1} and modulated cooling at an average rate of 2 °C min^{-1}. The corresponding thermal data, glass transition, crystallisation and melting temperatures, enthalpies and crystallinity, are listed in Table 1. A single melting peak in the range of 168–174 °C was observed for all samples, except for the samples treated at 2 and 10 °C min^{-1} rates. These samples showed a melting peak with a shoulder that emerged from the higher temperature side of the melting peak (as indicated by an arrow). The sample cooled at a 2 °C min^{-1} rate (SC2-PHB) had a relatively sharper peak with the lowest T_m value (167.4 °C) and a shoulder at 172.5 °C, while PHB

Table 1
Thermal data of PHB samples treated by different cooling treatments

Polymer	T_g (°C)	T_{cc} (°C)	ΔH_{cc} (J g^{-1})	T_{m1} (°C)	T_{m2} (°C)	ΔH_m (J g^{-1})	X_c
FC200-PHB	0.03	46.4	47.9	173.1	–	81.0	0.56
CC10-PHB	–	–	–	168.2	173.2	103.9	0.71
SC2-PHB	–	–	–	167.4	172.5	92.5	0.63
HC2-PHB	–	–	–	171.2	–	86.0	0.59
IS2-PHB	–	–	–	171.4	–	97.4	0.67

FC200-PHB cool 200 °C min^{-1}, heat 10 °C min^{-1}; CC10-PHB cool 10 °C min^{-1}, heat 10 °C min^{-1}; SC2-PHB slow cool 2 °C min^{-1}, heat 10 °C min^{-1}; HC2-PHB heat–cool average rate 2 °C min^{-1}, heat 10 °C min^{-1}; IS2-PHB iso-scan average rate 2 °C min^{-1}, heat 10 °C min^{-1}.

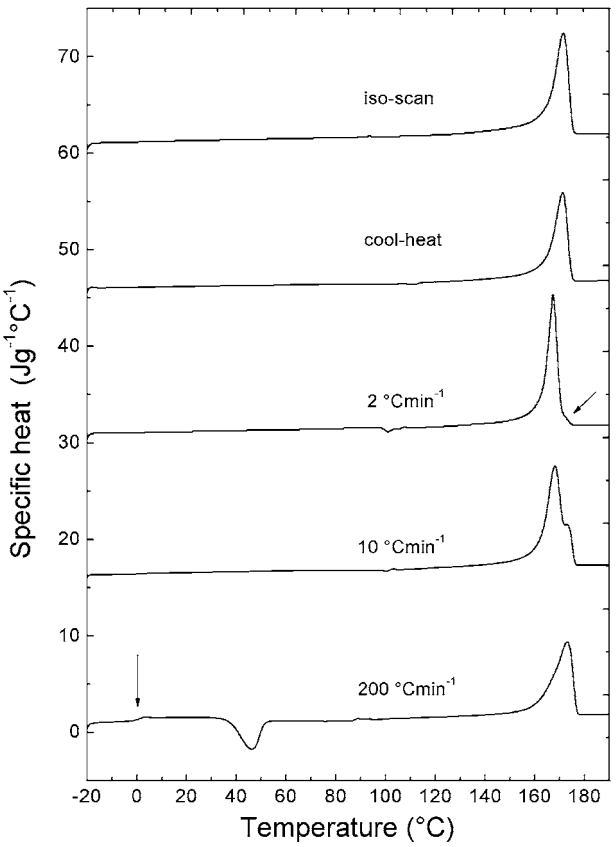

Fig. 1. DSC specific heat melting curves of PHB obtained at a rate of 10 °C min^{-1} after crystallising with various conditions. The crystallisation conditions (indicated on curves) involved fast cooling at 200 °C min^{-1}, slow cooling at 2 °C min^{-1}, moderate cooling at 10 °C min^{-1} and dynamic cooling at an average rate of 2 °C min^{-1} (an adapted scale is drawn by adding 15 units to each curve).

crystallised at 200 °C min^{-1} rate (FC200-PHB) showed a much broader peak with the highest T_m (173.1 °C). It can also be seen from Fig. 1 (last three curves) that as the cooling rate increases, melting peaks are shifted towards higher temperatures and peak becomes broader, indicating the melting may be accompanied by recrystallisation for the samples crystallised at faster rates. The recrystallisation process causes the development of the second melting peak during the DSC heating, while the first melting peak is due to formation of primary crystals during the cooling process.

The double or multiple melting behaviour is not uncommon for PHB and its copolymers depending on the crystallisation conditions [23]. Multiple melting behaviour of a polymer is usually proposed to link either to the process of partial melting and recrystallisation and remelting (mrr) or to melting of crystals with different lamellar thickness and/or different crystal structures [24]. It has been shown that mrr process is operative for melt-crystallised PHB [25]. The data also suggested that the extent of recrystallisation during heating was less for the SC2-PHB and CC10-PHB. Similar behaviour was reported by Chen et al. for PHB and maleated PHB as the cooling rates increases [25].

As seen in Table 1, CC10-PHB sample had the highest crystallinity (X_c, 0.71) and the FC200-PHB sample crystallised at a 200 °C min^{-1} rate had the lowest (0.56). The latter sample was rapidly cooled to create samples with lower initial crystallinity. As expected, the heating scan of FC200-PHB shows a glass transition (as marked on the curve) at about 0 °C and an exothermic cold crystallisation peak at 46 °C, suggesting the development of amorphous PHB during the extremely fast-cooled treatments [25]. In contrast, the highly crystalline PHB samples that were crystallised at rates of 10 °C min^{-1} or lower showed no T_g or cold crystallisation peaks in the DSC scans. The increased crystallinity of CC10-PHB may be due to the recrystallised and/or annealed PHB crystals during the melting scan.

Two cooling modulations were used to impart different thermal histories, a cool–heat cycle and an isothermal–cool cycle. It is also interesting to note that the PHB samples cooled by both temperature modulation methods gave single endothermic peaks (upper two curves in Fig. 1) with similar T_m (171 °C) values, but with different crystallinity. Again, the shift of T_m to a higher temperature and the presence of a broader peak indicated the occurrence of mrr process during heating. The crystallinity of the IS2-PHB sample (0.67) is rather higher than HC2-PHB (0.59) sample. Modulated cooling in a TMDSC has been known to anneal polymer crystals. Menzel has found that modulated cooling can be used to enhance the perfection of poly(*p*-phenylene sulphide) crystals formed during the conventional cooling from the melt, and the perfection is significantly improved by remelting and recrystallisation of outer lamella layers [26].

In the cool–heat cycle, the cooling step can initiate some crystallisation when the temperature is sufficiently low. During the heating part of the cycle, unstable crystals can melt, so that during the next cooling cycle the polymer has another opportunity to crystallise in a more stable way. Hence, the crystals formed at the end of all cycles are expected to be more stable than crystals formed during continuous cooling where the opportunity to re-melt and crystallise is limited. Under an iso-scan program, which contains a sequence of cooling and isothermal steps, the polymer has the opportunity to crystallise under isothermal conditions at a series of decreasing isothermal temperatures. Thus, the samples treated by iso-scan program had greater equilibration time than the samples from cool–heat method. Since iso-scan method allows more time for the rearrangement of unstable crystals. Therefore, the increased crystallinity of IS2-PHB compared with HC2-PHB could be attributed to the crystal perfection during the isothermal step. Polymers are often crystallised under isothermal or non-isothermal cooling conditions. Under isothermal conditions the perfection of the crystals is determined by the chosen temperature. Under non-isothermal cooling conditions, the formation and perfection of crystals are controlled by the cooling rate. However, under the step-wise conditions of modulated cooling, crystals can equilibrate.

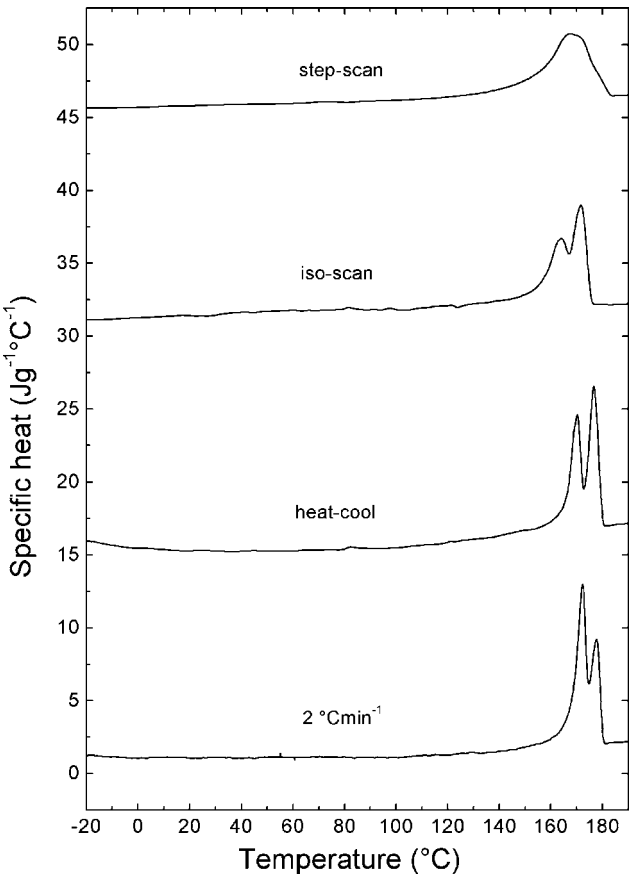

Fig. 2. DSC specific heat melting curves of PHB obtained from various melting programs after crystallising at a rate of 2 °C min^{-1}. The melting conditions (indicated on curves) involved continuous melting at 2 °C min^{-1} and dynamic melting at an average rate of 2 °C min^{-1} using TMDSC and SSDSC programs (an adapted scale is drawn by adding 15 units to each curve).

3.2. Influence of melting conditions

The behaviour of PHB under the various melting conditions was investigated. PHB samples were prepared by continuous cooling at a rate of 2 °C min^{-1} from 190 to −20 °C and analysed by using various melting conditions of conventional DSC, TMDSC (iso-scan and heat–cool) and step-scan DSC with an average heating rate of 2 °C min^{-1}. The melting curves are presented in Fig. 2 and the corresponding crystallinity, melting temperature and enthalpy values are listed in Table 2. Varied melting behaviour was observed under each heating profile. The sample (SC2-PHB-DSC2) analysed by conventional DSC program (continuous heating at a rate of 2 °C min^{-1}) had two sharp, but unresolved melting peaks. As discussed earlier, the lower melting peak at 172 °C may be due to the melting of primary crystals and the higher peak (178 °C) could be attributed to the melting of recrystallised crystals. Interestingly, the melting curve of the sample cooled at 2 °C min^{-1}, but heated at 10 °C min^{-1} (SC2-PHB, third curve in Fig. 1) showed single melting peak (167.4) with an overlapped shoulder at 172.5 °C, whereas

Table 2
Thermal data of PHB samples melted by various heating programs

Polymer	T_{m1} (°C)	T_{m2} (°C)	ΔH_m (J g^{-1})	X_c
SC2-PHB-DSC2	172.4	177.6	86.1	0.59
SC2-PHB-HC2	170.1	176.6	89.8	0.62
SC2-PHB-IS2	164.0	171.7	95.1	0.65
SC2-PHB-SSDSC2	167.5	170.4	98.2[a]	0.67

SC2-PHB-DSC2 cool 2 °C min^{-1}, heat 2 °C min^{-1}; SC2-PHB-HC2 cool 2 °C min^{-1}, heat–cool average rate 2 °C min^{-1}; SC2-PHB-IS2 cool 2 °C min^{-1}, iso-scan average rate 2 °C min^{-1}; SC2-PHB-SSDSC2 cool 2 °C min^{-1}, step-scan average rate 2 °C min^{-1}.
[a] ΔH_m is taken from thermodynamic C_p curve.

the PHB sample that was crystallised and melted at the rate of 2 °C min^{-1} (SC2-PHB-DSC2) gave clearly two melting peaks at 172.4 and 177.6 °C, supporting the phenomenon of recrystallisation during melting. The heating rate used was 2 °C min^{-1}, which is regarded as a relatively slow scan rate and at that rate PHB molecules would have enough time to undergo recrystallisation.

The PHB samples, crystallised at a 2 °C min^{-1} rate were also analysed by TMDSC. Fig. 2 displays the total specific heat melting curves obtained by both heat–cool and iso-scan modulation programs with an average heating rate of 2 °C min^{-1}, and the total C_p curve is suggested to give a similar level of information as does conventional DSC [27]. These melting curves also exhibited overlapped double melting endotherms, suggesting the presence of mrr process. Nevertheless, the PHB sample analysed by TMDSC heat–cool program gave better resolved double melting peaks appeared at 170 and 177 °C, while the melting peaks obtained from iso-scan program (SC2-PHB-IS2) showed much broader peaks (164 and 172 °C) at lower temperatures. In these curves, the area of the secondary crystal melting peak is higher than the primary crystal melting peak, suggesting the large degree of recrystallisation. The melting curve analysed by step-scan DSC heating program also demonstrates a very broad peak that contains two largely overlapped melting peaks (167 and 170 °C), indicative of significant recrystallisation during melting. As observed before, the crystallinity was higher for the modulated heating samples (Table 2), suggesting the annealing of crystals during the modulated heating. Further clarification of these curves can be obtained from Figs. 3 and 4.

Illustrated in Fig. 3a and b are the storage (reversing), loss, and non-reversing specific heat capacity curves derived from the TMDSC heat–cool and iso-scan melting scans, respectively. The corresponding data are listed in Table 3. The melting transition can be seen in all curves. The C'_p curve of SC2-PHB-HC2 sample shows three small melting peaks: a broad melting peak at about 162 °C followed by two melting peaks at 172 and 178 °C, while the NRC_p curve shows a broad exothermic peak before melting (indicated by arrow ∼150 °C) and two large melting endotherms. As mentioned previously, the reversing heat

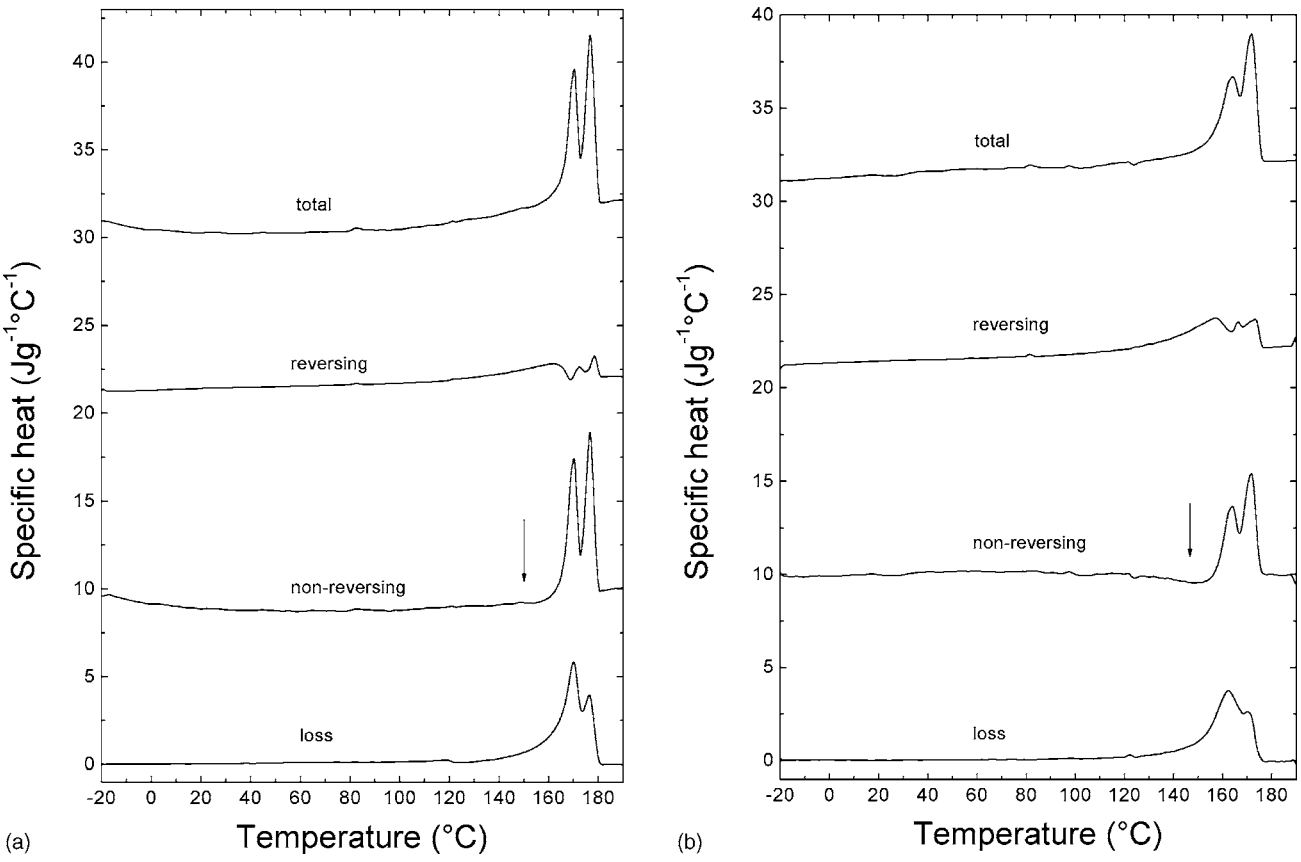

Fig. 3. Modulated specific heat curves of slow-cooled PHB obtained by (a) heat–cool and (b) iso-scan programs. Total specific heat, reversing specific heat, loss specific heat and non-reversing specific heat curves (indicated on curves) are shown (an adapted scale is drawn by adding 10 units to each curve).

capacity signal contains the reversible component of the total heat capacity, while the NR signal represents all irreversible component of the total heat capacity at the time and temperature of the modulation. The exothermic-only or both endothermic and exothermic behaviour of NRC_p curve has also been observed for other polymers such as poly(ethylene-2,6-napthalenedicarboxylate) [28,29] and polyethylenes [30,31] depending on the crystal stability. The presence of an exothermic NR contribution suggested that PHB experienced significant recrystallisation and/or annealing throughout the heating process. It is often not possible to detect the recrystallisation exotherm in the conventional DSC scan due to the offset of recrystallisation exotherm and melting endotherm. The loss specific heat curve, which also represents the irreversible contribution during the modulation, is a part of the NRC_p curve. It shows exactly zero baseline up to 120 °C, suggesting there is no structural changes involved before that temperature.

The analogous melting behaviour was also observed in the corresponding C'_p curves for the sample scanned using TMDSC iso-scan program (Fig. 3b), but displayed a much broader endothermic signal. Similarly, the corresponding NRC_p curves of SC2-PHB-IS2 sample illustrated that certain exothermic activity was also involved before

Table 3
TMDSC data of polymers after different melting conditions

Polymer	T_m (total C_p) (°C)	ΔH_m (total C_p) ($J\,g^{-1}$)	T_m (C'_p) (°C)	ΔH_m (C'_p) ($J\,g^{-1}$)	T_m (NRC_p) (°C)	ΔH_m (NRC_p) ($J\,g^{-1}$) (°C)	T_m (C''_p)	ΔH_m (C''_p) ($J\,g^{-1}$)
SC2-PHB-HC2	170.1 176.6	89.8	162.1 172.2	26.0	170.2 176.6	63.8	170.0 176.2	79.8
SC2-PHB-IS2	164.0 171.7	95.1	157.3 166.1	49.0	164.1 171.7	46.1	162.2 170.2	71.0
SC2-PHB-SSDSC2	–	–	167.5[a] 170.4	98.2	169.5 176.0	14.5	–	–

[a] T_m is taken from thermodynamic C_p curve.

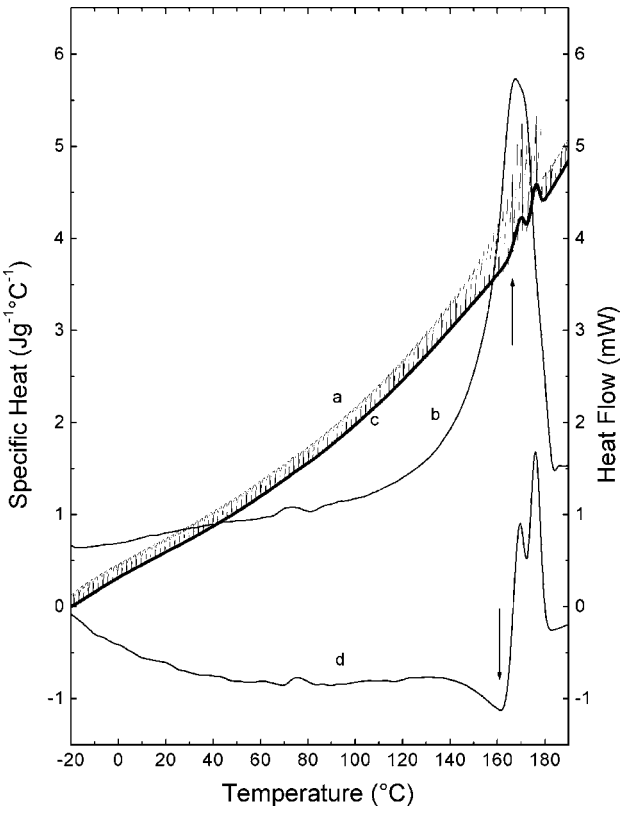

Fig. 4. (a) Raw heat flow, (b) thermodynamic C_p, (c) IsoK baseline and (d) IsoK baseline (corrected) of SC2-PHB from the SSDSC experiment.

the melting of PHB. The enthalpies of reversing and NR components are shown in Table 3. It can be seen that the reversing contribution is significantly smaller than the non-reversing contribution, indicating that PHB sample had perfect crystals. It has been known that poorly crystallised polymers have a larger reversing melting contribution and smaller NR contribution, while perfect crystals show a little or none has smaller reversing and larger NR contributions [11]. Analogous results has been reported for the TMDSC studies of poly(ethylene succinate) and poly(butylene succinate) biopolymers by Qiu et al. [32]. Endothermic melting can be detected in both reversing and non-reversing specific heat curves. But, exothermic behaviour is detected only in the non-reversing specific heat capacity curve because the slow kinetics cause a heat flow response, which is not in-phase with the temperature oscillation [11]. Stable primary crystals contribute to melting, which is fully reversible in the reversing curve because it is in-phase with the modulation.

SSDSC scan results the raw heat flow, thermodynamic C_p and IsoK baseline curves (curves a, b and c, respectively), shown in Fig. 4. The thermodynamic C_p curve, which is similar to reversing C_p shows only thermodynamic changes during the heating while the IsoK baseline or non-reversing C_p clearly represents the kinetic changes of the sample [17]. Both IsoK baselines (corrected (curve d) and uncorrected) reveal that PHB may undergo some recrystallisation during melting, as is evidenced by the exothermic peaks (indicated by an arrow). The IsoK baseline is similar to the non-reversing curve shown in Fig. 3b obtained using iso-scan TMDSC, in that there is an exotherm followed by a double melting endotherm of similar shape in each curve. The step-scan method does not involve a Fourier transform, it uses the approach to equilibration during the isothermal region of each step to obtain the IsoK, or kinetic, contribution. As in TMDSC, the endothermic melting is also evident in both thermodynamic C_p and IsoK baseline signals [17]. Therefore, SSDSC data supported that the presence of melting–recrystallisation–remelting process.

3.3. Morphological studies

Hot stage optical microscopy (HSOM) provide a direct view of the polymer during crystallising, while DSC results give an indirect view of the physical changes as it is heated, cooled or maintained under isothermal conditions. The crystal morphologies of PHB with various treatments were observed by polarised optical microscopy. As seen in Fig. 5, different crystal morphologies were obtained under various crystallisation conditions. All images showed the characteristics large spherulites that contain Maltese cross-birefringent pattern and concentric extinction bands [19]. A sharp fibril structure growing radially with large radius was seen for the isothermally crystallised PHB at 80 °C (Fig. 5a). Both images in Fig. 5b and c showed characteristic concentric bands; however the higher nucleation density was noticed for CC10-PHB. Slow cooling permitted larger crystals with lower nucleation density compared with faster cooling that showed smaller crystal size with increased nucleation density. Furthermore, the fast-cooled samples showed larger band spacing compared with slow cooled samples.

Fig. 5d shows the OM images obtained after stepwise isothermal crystallisation (isothermal crystallisation at 140, 120 and 90 °C). This was performed to mimic the TMDSC iso-scan cooling behaviour. At 120 °C, uniform small crystals appear; but not covering all the area due to the slow growth rate at this temperature. No crystals were appeared at 140 °C, since PHB was in the melt. In order to see the details of morphology development after the third isothermal step at 90 °C. These findings are consistent with the large individual spherulites of PHB previously observed [1,19]. Separation of bands and regularity of bands varied with crystallisation temperatures and conditions [33,34]. Isothermal and slow-cooled samples provided a large average radius of the spherulites indicating a low nucleation density [8]. It is these large spherulites that are responsible for the brittleness of PHB [20]. These results provided clear evidence of crystal growth dependence of PHB under different crystallisation conditions using TMDSC techniques.

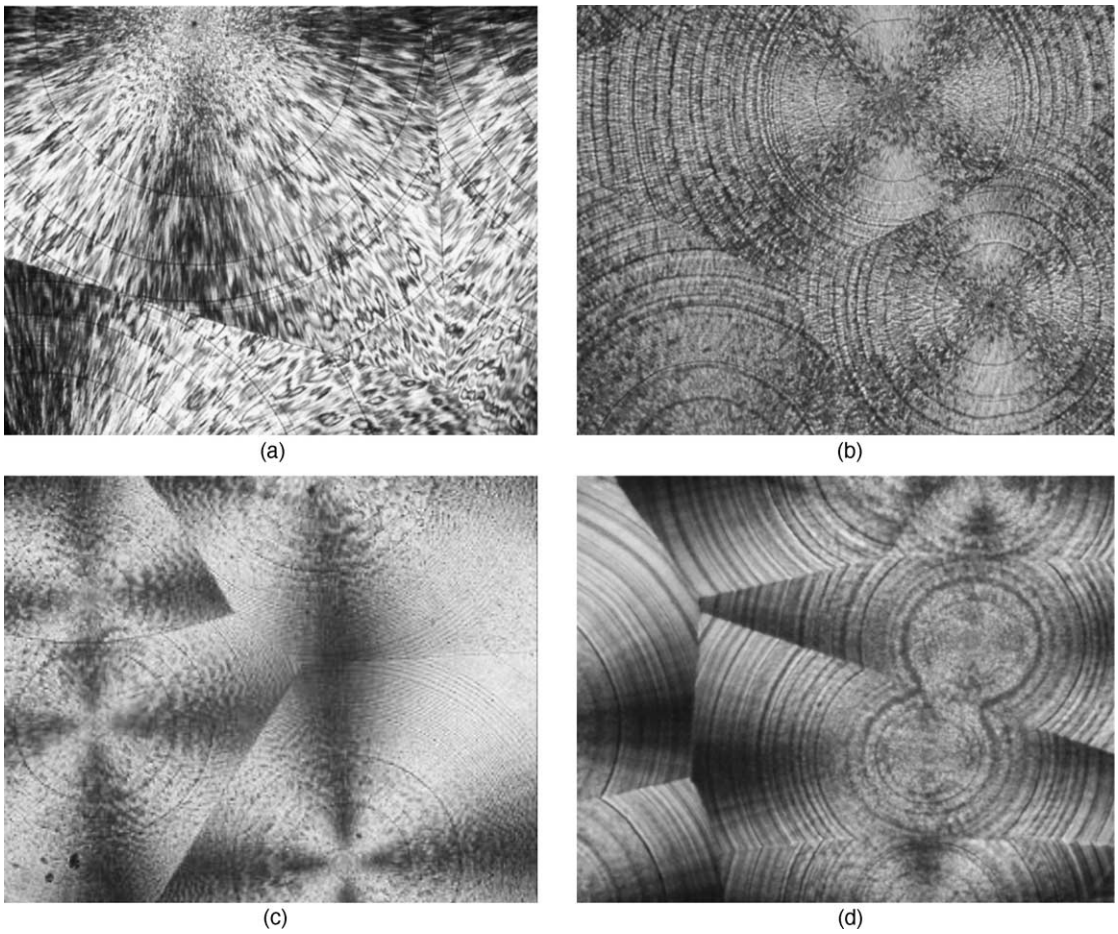

Fig. 5. Polarised optical micrographs (magnification 100×) of PHB after various cooling treatments: (a) isothermal crystallisation at 80 °C; (b) continuous cooling at 2 °C min^{-1}, (c) continuous cooling at 10 °C min^{-1} cooling, (d) at 90 °C after three-step cooling.

4. Conclusions

PHB has been crystallised using various non-isothermal cooling profiles including TMDSC cool–heat and cool–isothermal step-wise programs. Subsequent melting behaviour of these samples revealed that all samples experienced secondary crystallisation during heating and the extent of secondary crystallisation was varied depending on the treatment. SC2-PHB and CC10-PHB samples undergo less recrystallisation, while FC200-PHB gave amorphous PHB with lower crystallinity. Considerable secondary crystallisation/annealing was noticed for the samples treated with modulated cooling conditions. Moreover, the effect of melting conditions was also investigated by applying various continuous and modulated programs. The overall melting behaviour was rationalised in terms of recrystallisation and/or annealing of crystals. Interestingly, the samples analysed by temperature modulation programs showed a broad exotherm before the melting peak in the non-reversing curve and a multiple melting reversing curve, verifying that the melting–recrystallisation and remelting process is also operative. Various crystal morphologies obtained by HSOM confirmed the thermal history effect on PHB.

References

[1] A. Ei-Hadi, R. Schanabel, E. Straube, G. Muller, S. Henning, Polym. Test. 21 (2002) 665–674.
[2] C.S. Ha, W.J. Cho, Prog. Polym. Sci. 27 (2002) 759–809.
[3] K. Van de Velde, P. Kiekens, Polym. Test. 21 (2002) 433–442.
[4] X. Shuai, F.E. Porbeni, M. Wei, T. Bullions, A.E. Tonelli, Macromolecules 35 (2002) 3126–3132.
[5] A.A. Mansour, G.R. Saad, A.H. Hamed, Polymer 40 (1999) 5377–5391.
[6] H. Marand, A. Alizadeh, R. Farmer, R. Desai, V. Velikov, Macromolecules 33 (2000) 3392–3403.
[7] R.E. Withey, J.N. Hay, Polymer 40 (1999) 5147–5152.
[8] M. Gazzano, M.L. Focarete, C. Reikel, A. Ripamonti, M. Scandola, Macromol. Chem. Phys. 202 (2001) 1405–1409.
[9] P.S. Gill, S.R. Sauerbrunn, M. Reading, J. Therm. Anal. Calorim. 40 (1993) 931–939.
[10] J.E.K. Schawe, Thermochim. Acta 260 (1995) 1–16.
[11] B. Wunderlich, I. Okazaki, K. Ishikiriyama, A. Boller, Thermochim. Acta 324 (1998) 77–85.
[12] B. Wunderlich, A. Boller, I. Okazaki, K. Ishikiriyama, W. Chen, M. Pyda, J. Pak, I. Moon, R. Androsch, Thermochim. Acta 330 (1999) 21–38.
[13] S.L. Simon, Thermochim. Acta 374 (2001) 55–71.
[14] M. Sandor, N.A. Bailey, E. Mathiowitz, Polymer 43 (2002) 279–288.
[15] M. Reading, R. Luyt, J. Therm. Anal. 54 (1998) 535–544.

[16] G. Amarasinghe, F. Chen, A. Genovese, R.A. Shanks, J. Appl. Polym. Sci. 90 (2003) 681–692.
[17] K. Pielichowski, K. Flejtuch, J. Pielichowski, Polymer 45 (2004) 1235–1242.
[18] G.J.M. de Koning, P.J. Lemstra, D.J.T. Hill, T.G. Carswell, J.H. O'Donnell, Polymer 33 (1992) 3295–3297.
[19] F. Biddlestone, A. Harris, J.N. Hay, Polym. Int. 39 (1996) 221–229.
[20] P.J. Barham, A. Keller, J. Polym. Sci.: Polym. Phys. Edit. 24 (1986) 69–77.
[21] L.L. Zhang, S.H. Goh, S.Y. Lee, G.R. Hee, Polymer 41 (2000) 1429–1439.
[22] S. Gogolewski, M. Jovanovic, S.M. Perren, J.G. Dillon, M.K. Hughes, J. Biomed. Mater. Res. 27 (1993) 1135–1148.
[23] R. Pearce, R.H. Marchessault, Polymer 35 (1994) 3990–3997.
[24] V.B.F. Mathot (Ed.), Calorimetry and Thermal Analysis of Polymers, Hanserm, New York, 1993, pp. 231–299.
[25] C. Chen, B. Fei, S. Peng, Y. Zhuang, L. Dong, Z. Feng, Eur. Polym. J. 38 (2002) 1663–1670.
[26] J.D. Menczel, J. Therm. Anal. Calorim. 58 (1999) 517–523.
[27] Y. Jin, J. Bonila, Y.G. Lin, J. Morgan, L. McCracken, J. Carnahan, J. Therm. Anal. 46 (1996) 1047–1059.
[28] B.B. Sauer, W.G. Kamper, E.N. Blanchard, S.A. Threefoot, B.S. Hsiao, Polymer 41 (2000) 1099–1108.
[29] W.G. Kampert, B.B. Sauer, Polymer 42 (2001) 8703–8714.
[30] R. Scherrenberg, V. Mathot, A.V. Hemelrjk, Thermochim. Acta 330 (1999) 3–19.
[31] J. Pak, B. Wunderlich, Macromolecules 34 (2001) 4492–4503.
[32] Z. Qiu, M. Komura, T. Ikehara, T. Nishi, Polymer 44 (2003) 7781–7785.
[33] A. Keller, H.H. Willis, J. Polym. Sci. XXXIX (1959) 151–173.
[34] S.J. Organ, P.J. Barham, J. Mater. Sci. 26 (1991) 1368–1374.